

In Situ Synchrotron Powder Diffraction Studies of Reduction–Oxidation (Redox) Behavior of Iron Ores and Ilmenite



ALEXANDER Y. ILYUSHECHKIN, MARK KOCHANNEK, LIANGGUANG TANG,
and SENG LIM

Phase transformations of two types of iron-based oxides (iron ore and industrial-grade ilmenite) were studied using synchrotron powder diffraction of the samples processed in reducing and oxidizing atmospheres at 1173 K (900 °C) and 1223 K (950 °C), respectively. In iron ore oxidation, the disappearance of the wustite and fayalite phases was followed by hematite growth and a decrease of the magnetite phase. The magnetite phase was partially recovered by treatment in a reducing atmosphere. Ilmenite oxidation initiated decomposition of the ilmenite phase with rapid growth of hematite and gradual growth of the pseudobrookite phase. In a reducing atmosphere, ilmenite was gradually recovered from pseudobrookite with a relatively fast initial decrease in rutile and hematite content. Under reducing conditions, there was interaction of iron ore with magnesio-ferrites in iron ore–ash mixture and interaction of ilmenite with silica by the formation of fayalite.

DOI: 10.1007/s11663-017-0919-7

© The Minerals, Metals & Materials Society and ASM International 2017

I. INTRODUCTION

CHEMICAL looping combustion (CLC) is an attractive option for processing different feedstocks in an environmentally friendly manner, as it allows the consequent capture of carbon from the combustion processes.^[1,2] A key component of CLC are the metal oxides, called oxygen carriers (OCs), which provide the oxygen for combustion by the reduction reaction. After reduction, the oxides are converted to their initial valency state and then are oxidized to their initial state in a separate reactor. Effective OCs in CLC processes must be highly reactive with the fuel, have a high oxygen capacity, be non-toxic, and be capable of fast redox reactions without losing mechanical strength or agglomeration.^[3]

In the past decade, a number of materials have been tested as potential OCs for CLC. Of these, industrial-grade, iron-based OCs are relatively cheap, environmentally friendly, and generally demonstrate good reactivity with CO and H₂.^[2,4] While these oxides have been investigated for their application in CLC using a number of pilot-scale fluidized fuel and air reactors,^[4–6] laboratory techniques are still important, as they enable differentiation of the factors affecting OC performance in CLC systems. For example, to help design pilot tests, it is important to evaluate the

reduction and oxidation behavior of OCs and determine their characteristics, such as reactivity, microstructure, and mechanical strength, in the laboratory.

In our previous studies,^[7,8] the kinetics of the oxidation and reduction of ilmenite and iron ore, with and without Australian brown coal ashes, was investigated using thermogravimetric analysis (TGA) and post-run X-ray diffraction (XRD) analysis. Tube furnace experiments, along with electron microscopy of the processed samples, were also used to investigate the impact of coal ash and cycling of the materials on their microstructure and phase transformations. Electron microscopy with an electron probe microanalyzer (SEM–EPMA) enabled changes after processing to be detected, and local interactions of coal ash with ilmenite and iron ore were observed. Cyclic treatment and the presence of ash affected the kinetics of the reduction and oxidation. However, the mechanism of the reaction was not fully studied, as TGA provides overall mass changes in the oxide's system, and the kinetics may also be affected by interaction with the support materials. Additionally, in all experiments, oxides were processed in CO atmosphere (not in direct contact with carbon), which may also affect the kinetics of the reaction.

As a continuation of the laboratory testing of OC, we apply the synchrotron powder diffraction technique to gain further insights into the material reactions occurring during CLC processes. Among the analytical methods available to study microstructural changes at high temperatures in oxide systems, synchrotron powder diffraction is an effective tool to investigate *in situ* phase transformation, particularly during an oxide's reduction and oxidation. The method has been previously used to identify the changes in iron oxide systems during heat treatment: goethite–hematite transformation during calcination were investigated in air at temperatures in the

ALEXANDER Y. ILYUSHECHKIN and MARK KOCHANNEK are with the Queensland Centre for Advanced Technologies, CSIRO Energy, 1 Technology Court, Pullenvale, QLD 4069, Australia. Contact e-mail: alex.ilyushechkin@csiro.au LIANGGUANG TANG and SENG LIM are with the Queensland Centre for Advanced Technologies, CSIRO Energy, CESRE Bushells Building, 71 Normanby Road, Clayton North, VIC 3169, Australia.

Manuscript submitted September 13, 2016.

Article published online January 23, 2017.

range of 298 K to 1073 K (25 °C to 800 °C).^[9] The phase transformations of ilmenite were investigated at temperatures up to 1123 K (850 °C) under reducing conditions.^[10,11] Transformations of hematite to magnetite were investigated, where Fe₂O₃–coal mixture was heated up to 1223 K (950 °C) in CO₂. The reverse transformation in an oxidizing atmosphere were also studied^[12]; however, the kinetics and mechanism of the transformation was not discussed. In the present study, we simulate CLC reducing and oxidizing conditions to investigate *in situ* changes in phase content and understand the reactions in ilmenite and iron ore systems. At the same time, we identify the minor phases of the reaction products in the ash–OC mixture—these are difficult to identify by conventional XRD due to overlapping of XRD peaks and the low intensities.

II. EXPERIMENTAL

A. Materials

Industrial-grade iron ores (OC1 and OC2, both are hematite–goethite mixtures) and ilmenite (OC3) were used as raw materials for OCs and were initially crushed to obtain particle sizes of <250 μm. To study the reduction kinetic using synchrotron powder diffraction, these materials were preliminary heat-treated in air in a muffle furnace at 1173 K (900 °C) for 5 hours. For each OC, the subsamples (second set of samples) were then heat treated in a tube furnace at 1173 K (900 °C) for 10 hours in graphite lining under a neutral atmosphere (in N₂ flow) that simulated reducing conditions. This set was used to study the kinetic of oxidation. The third set of materials was mixed with coal ash (2:1 ratio) and graphite (20:1 ratio) after air heat treatment, to investigate the phase changes during the redox cycle in the presence of coal mineral matters. This simulated the compositional changes occurring in OC during brown coal CLC.

B. In Situ X-ray Diffraction Measurements

Samples were loaded into 0.7-mm OD amorphous fused quartz capillaries, connected to a gas supply line (N₂ or air), and the capillaries were oscillated during measurements. The capillaries were heated using a hot gas blower mounted perpendicular to the X-ray beam at a distance of 3 mm from the capillary wall. Measurements were made at the Australian Synchrotron (Melbourne, Australia), using the powder diffraction beamline. The wavelength used was 0.8248 Å.

In the experiments studying materials' oxidations, one set of samples was quickly heated up to 773 K (500 °C) in nitrogen flow (60 mL/minute), and then heated up to 1223 K (950 °C) at 10 °C/minute with XRD patterns taken in intermediate temperatures, and then the gas was switched to air. Second set of samples, flushed in N₂ flow, were inserted in a hot gas blower in order to eliminate oxidation reaction at low temperatures. After taking the first XRD data, the gas was switched to air (30 mL/minute). XRD patterns were taken at 1.2 to 3.5 minute intervals for 30 to 60 minute.

In the experiments simulating reduction–oxidation reactions, the mixtures, flushed in N₂ flow, were inserted

in a hot gas blower at 900 °C and kept for 25 minute, and then the temperature was increased to 1223 K (950 °C) and the gas was switched to air. The samples were kept at 1223 K (950 °C) for another 35 minute and XRD patterns were taken with 3.5-minute intervals.

C. Material Analysis

The bulk composition of coal ashes and OC composition were determined by X-ray fluorescence (XRF) according to the ASTM D3174-12 standard and are listed in Table I.

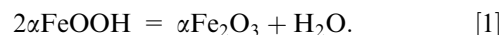
HighScore Plus software was used to identify phase compositions in powder diffraction patterns and to calculate phase content in the samples.^[13] The separate calculation on phase content was also performed using peak ratios only and the results were compared.

Samples microstructures were observed using JEOL 8200 electron probe.

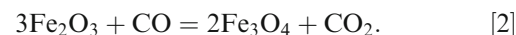
D. Reactions

Based on the thermodynamics of iron oxide systems under the oxidizing and reducing conditions used in this study, the following reactions are expected.

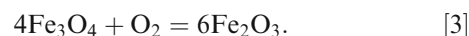
During iron ore calcination, at temperatures above 473 K (200 °C), goethite starts to decompose to hematite and water and is completely decomposed at temperatures above 973 K (700 °C)^[4]:



Then, hematite is reduced with the formation of spinel magnetite^[4]:



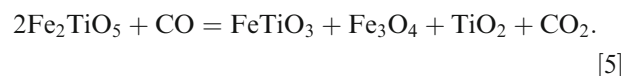
Following oxidation, magnetite converts back to hematite:



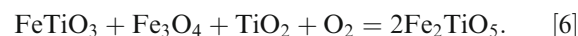
In the ilmenite system, calcination converts ilmenite to ferric pseudobrookite and rutile:



In a reducing atmosphere, pseudobrookite leads to the formation of ilmenite, magnetite, and rutile^[15]:



Rutile, magnetite, and ilmenite are oxidized back to pseudobrookite:



III. RESULTS

A. Material Characteristics

The XRD of the raw materials are shown in Figure 1. Iron ores have hematite (Fe₂O₃) and goethite [FeO(OH)]

Table I. Chemical Composition (Wt Percent) of Oxygen Carriers and Coal Ashes, Determined by X-ray Fluorescence

	Fe ₂ O ₃	Al ₂ O ₃	SiO ₂	Mn ₃ O ₄	MgO	CaO	TiO ₂	Na ₂ O	K ₂ O	SO ₃
OC1	96.0	1.3	2.3	0	0	0	0	0	0	0
OC2	91.2	2.19	6.06	0.2	0.1	0.1	0.12	0	0	0
OC3	47.9	0.6	0.5	1.57	1.0	0	51.0	0	0	0
Bca1	45.1	1.7	3.2	0.5	18.5	7.3	0.1	5.2	0.4	16.7
Bca2	3.6	10.3	76.7	0	2.2	1.1	0	1.8	0.4	2.8

OC: oxygen carriers, Bca: coal ashes.

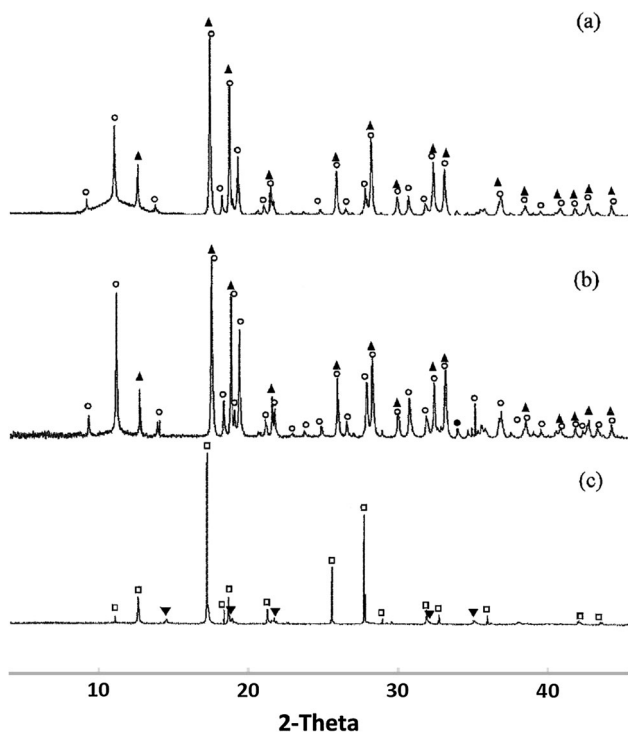


Fig. 1—Phase compositions of raw materials: iron ores OC1 (a) and OC2 (b), and ilmenite, OC3 (c). Legend: filled up pointing triangles Fe₂O₃, open circles Fe(OH)₂, open squares FeTiO₃, filled down pointing triangles TiO₂.

as their major phases, with weight ratios of 67:33 and 47:53 for OC1 and OC2, respectively, according to HighScore calculations. The ilmenite raw sample (OC3) had 93 wt pct ilmenite (FeTiO₃) and 7 wt pct rutile (TiO₂), which agrees with the chemical composition obtained by XRF listed in Table I.

After initial heat treatment in air, the surface area of raw materials was reduced for all OCs, especially for ilmenite, which had more than 10-fold surface decrease (Table II). Reduction treatment significantly decreased surface area in iron ore further, but did not affect ilmenite. A further decrease in surface area was observed in all samples after following oxidation. This possibly indicates that sintering and densification is more significant in initial oxidation for ilmenite and during transformation of hematite to magnetite (reduction step) in iron ores.

Figure 2 shows microstructures of iron ore sample (OC2) and ilmenite (OC3) after different stages of treatment: after initial oxidation (a, d), after reduction

(b, e), and after followed oxidation (c, f). This demonstrates that while initially oxidized OC2 has dense and microporous areas (Figure 2(a)), the reduced OC2 has larger pores (macroporosity) and dense grains (Figure 2(b)), with similar microstructure in the sample after followed oxidation (Figure 2(d)). Ilmenite has a dense microstructure after initial oxidation, which supports surface area analysis results. Cracking in the particles was observed in OC2 after reduction step, as well as in the particle after followed oxidization (Figures 2(b) and (c)), while in OC3 particle cracking was observed only after full redox cycle (Figure 2(f)).

B. In Situ Phase Transformations

1. Phase transitions in iron ore

The transformation of both iron ores during the initial oxidation was rapid. Only hematite was detected in the first recorded run at 773 K (500 °C), as well as the first 1223 K (950 °C) run when the sample was quickly inserted in the hot zone. Figures 3(a) and 3(b) demonstrates that the decomposition of FeOOH leads to transformation to hematite, as given in Eq. [1]. After treatment at reducing conditions, iron ores have mostly magnetite phase with some amounts of wustite, FeO, and hematite in OC1, and wustite and fayalite, Fe₂SiO₄ (due to silica impurity). Compositional changes in the reduced sample OC2 during following oxidation at 1223 K (950 °C) are shown in Figure 4. The treatment leads to disappearance of wustite and fayalite, reduction of the magnetite fraction, and an increase in hematite.

The phase composition changes during the oxidation treatment calculated by HighScore are shown in Figure 5(a), which demonstrate a parabolic hematite growth approximately 5 minute after treatment started. Hematite growth was nearly completed after 25 minute of oxidation. However, the accuracy of HighScore calculations, especially where peaks are overlapped could be affected by shifts in the peaks' positions due to the temperature.

Therefore, the phase changes in the sample were also validated using selected peaks height of XRD for each phase. The peaks used were: 17.4 deg for hematite, 21.9 deg for wustite, 22.4 deg for magnetite, and 26.6 deg for fayalite. Results of these calculations (Figure 5(b)) demonstrate similar phase relations, but the changes in phase content are smoother than those calculated by HighScore. In both graphs, wustite and fayalite disappeared after 8 and 14 minutes of oxidation, respectively, accompanied by fast growth of hematite and decreasing magnetite content.

Table II. Surface Area of Oxygen Carriers

N ₂ SA BET (m ² /g)	OC1	OC2	OC3
As received	4.35	7.84	1.96
Calcined	3.63	2.91	0.16
Reduced	0.4	0.5	0.15
Oxidized	0.24	0.3	0.08

When the OC2 sample in capillary with N₂ flow was inserted into the hot zone at 773 K (500 °C) and heated up to 1223 K (950 °C), the oxidation had already started and wustite peaks had completely disappeared with decreasing of magnetite phase content and increasing hematite phase content (Figure 6(a)). When the atmosphere changed to air at 1223 K (950 °C), the oxidation occurred mostly in first 8 minutes of the treatment (Figure 6(b)).

Oxidized iron ore samples were also exposed to a reduction–oxidation cycle in the presence of high-iron ash that mainly contains magnesio-ferrites. Firstly, the samples were exposed at 1173 K (900 °C) in a reducing atmosphere for 25 minutes. As shown in Figure 7, the hematite reduction occurred in first 8 minutes in sample OC1, and in first 14 minutes in sample OC2. It likely stopped due to a lack of carbon. The continuation of N₂ passing through the OC1 sample lead to a decrease in magnetite and some magnesio-ferrite growth. However, most of the magnesio-ferrite peaks overlapped with magnetite peaks. Therefore, an estimation by peak intensity of selected reflections for each phase was also made. The peaks selected for evaluation were 17.4 deg for hematite and 22.4 deg for magnetite. This demonstrated (Figure 7(c)) a slow magnetite decrease along with slow hematite growth. When the temperature was increased to 1223 K (950 °C) and the atmosphere switched to air, the hematite reached the initial concentration in 5 to 8 minutes. The final hematite/magnetite ratio based on the intensity of the selected peaks became even higher than the starting composition. Similar behavior was observed for sample OC2 (Figure 7(d)); however, most hematite growth and magnetite decrease occurred before the atmosphere was changed to air.

2. Phase transitions in ilmenite

Heat treatment of ilmenite in air at 1223 K (950 °C) leads to decomposition of the ilmenite phase (FeTiO₃) and growth of rutile (TiO₂), FeTi₂O₅ and hematite (Fe₂O₃). The main difficulty with quantitative phase identification is the overlapping peaks. For example, as shown in Figure 8, the main ilmenite peaks at 17.1 and 25.3 deg overlap with the 17.3 and 25.5 deg pseudobrookite peaks, and the 17.35 and 25.5 deg hematite peaks, and the ilmenite peak at 32.3 deg overlaps with the 33.5 deg hematite and rutile peaks. There are also a number of candidates for ilmenite, pseudobrookite, and other phases in the HighScore database and they have some variation in their peak positions. In addition, peak shift is observed for analyzed materials at high temperatures. All of these factors significantly affect the quantification of phase content. A similar approach

was taken to identify phase changes in iron ore, by selecting individual non-overlapping peaks, and monitoring their intensity during the reaction. For the OC3 sample, the peaks selected were 12.7 deg for Fe₂O₃, 13.5 deg for FeTi₂O₅, 14.5 deg for TiO₂, and 17.2 deg for FeTiO₃. Figure 9(a) shows changes in peak intensities of the major phases in the sample OC3 calcined at 1223 K (950 °C) in air. In multiphase samples, changes in intensities most commonly are related to the amount of each phase present in the sample.^[16] According to the figure, ilmenite decomposes in first 8 minutes of the calcination, leading to growth of rutile and hematite. After 13 minutes of calcination, pseudobrookite phase starts to crystallize. This demonstrates that transformation of ilmenite to pseudobrookite is a multistep process.

OC3 material (initially oxidized) converts to the ilmenite phase with some amounts of hematite, rutile, and titanium magnetite (Fe_{2.25}Ti_{0.75}O₄) after reduction in tube furnace at 1173 K (900 °C) for 10 hours in graphite lining. When this sample was heated up in capillary in N₂ flow to 1223 K (950 °C), all magnetite peaks disappeared between 773 K and 1173 K (500 °C to 900 °C) and ilmenite transforms to ilmenite–hematite solution with stoichiometry Fe_{1.35}Ti_{0.65}O₃. Figure 9(b) shows transformation of ilmenite–hematite to pseudobrookite and hematite, followed by a continued crystallization of pseudobrookite with some hematite consumption.

Reduction–oxidation cycle was taken for OC3 sample in the presence of silica-rich ash. Similar to iron ore, the reduction of OC1 and formation of ilmenite phase was limited by the volume of carbon in the sample and mainly occurred in first 15 minutes. It was accompanied by a gradual decrease of the pseudobrookite phase, while the reduction of hematite and rutile fractions mainly occurred in first 5 minutes (Figure 10).

C. Interaction of Iron Ore and Ilmenite with Ash

Previously, we observed local interactions of iron ore (sample OC1) with high-iron and magnesia ashes by SEM–EPMA analysis of the processed samples.^[8] During reduction, the mixtures had solid solutions of magnetite and magnesio-ferrite, assuming that magnetite is of iron ore origin. In the present work, we observed decreasing amounts of magnesio-ferrites in the reduction step, followed by an increase in their fraction in the mixture during oxidation. This supports the previous assumption that magnesia-ferrites could be transferred to magnetite. It is difficult to assess the transformation of Mg oxides, as it may still be part of magnetite or released as periclase (MgO). However, it is difficult to differentiate MgO peaks as they all overlapped with other phases (Figure 11).

The interaction of ilmenite with silica-rich ash was also detected by powder diffraction during reduction. Figure 12 shows growth of fayalite peaks after processing sample OC1 at 1223 K (950 °C). Those peaks disappear later in the oxidation step, which is similar to decomposition of fayalite during iron ore oxidation (as shown in Figure 5). The interaction between ilmenite and silica was previously observed, where the particles

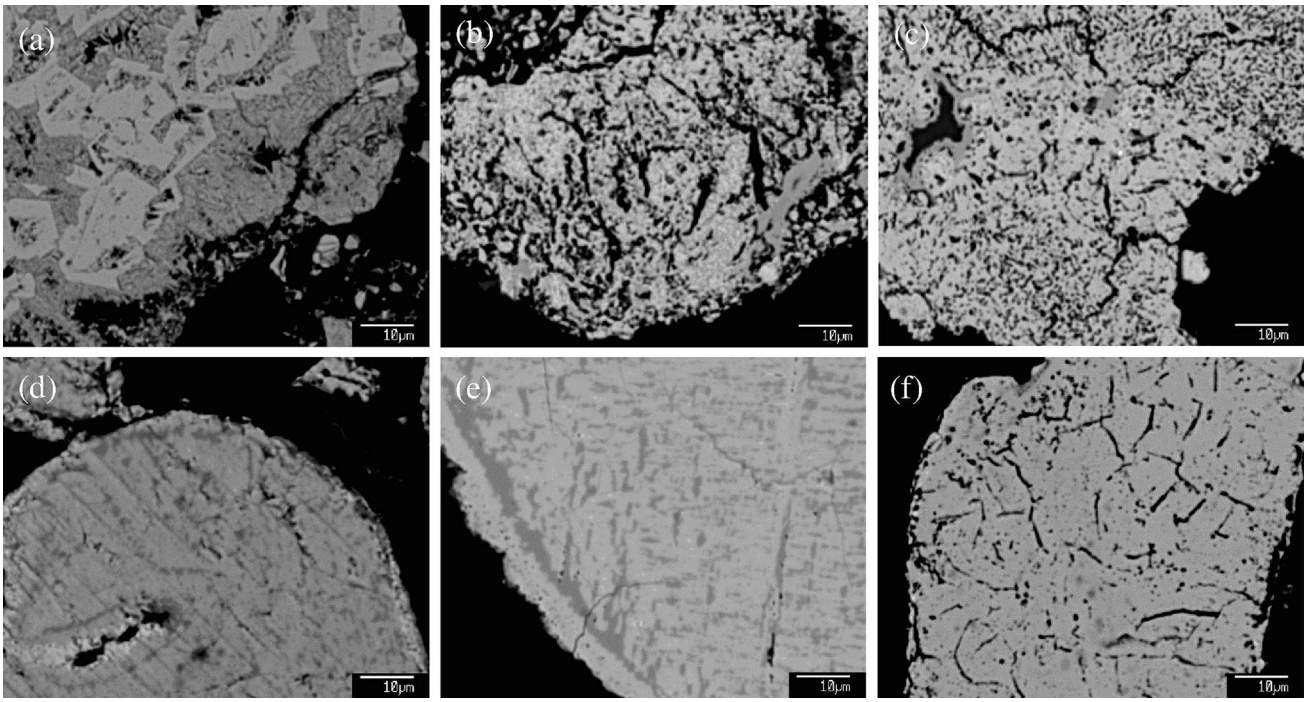


Fig. 2—Microstructures of OC2 (*a-c*) and OC3 (*d-f*) after different stages of treatment: after initial oxidation (*a, d*), after reduction (*b, e*), and after followed oxidation (*c, f*).

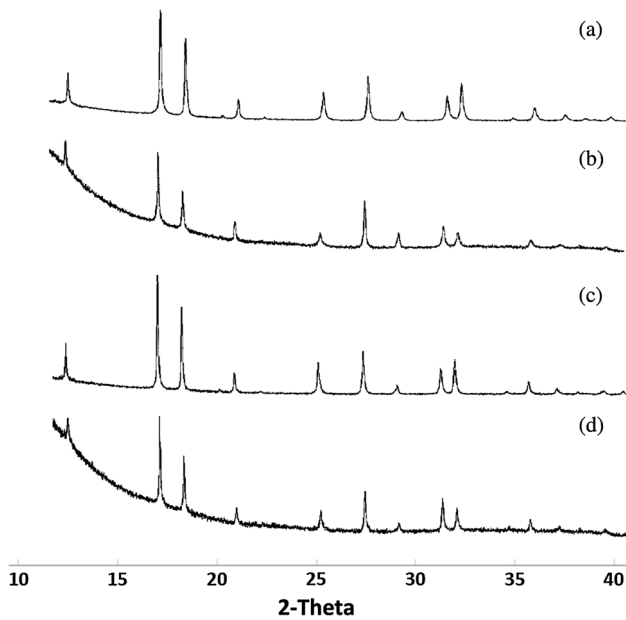


Fig. 3—Powder diffraction pattern of iron ore OC1 (*a*) and OC2 (*b*) at 773 K (500 °C), and OC1 (*c*) and OC2 (*d*) at 1223 K (950 °C). All peaks are from hematite.

were locally bonded by inter-diffusion or by formation of the liquid phase near interface. The samples were exposed for a longer period (5 hours) than in the present study, where formation of fayalite is probably the first step of the ilmenite–silica interaction. However, longer observation is required for confirmation.

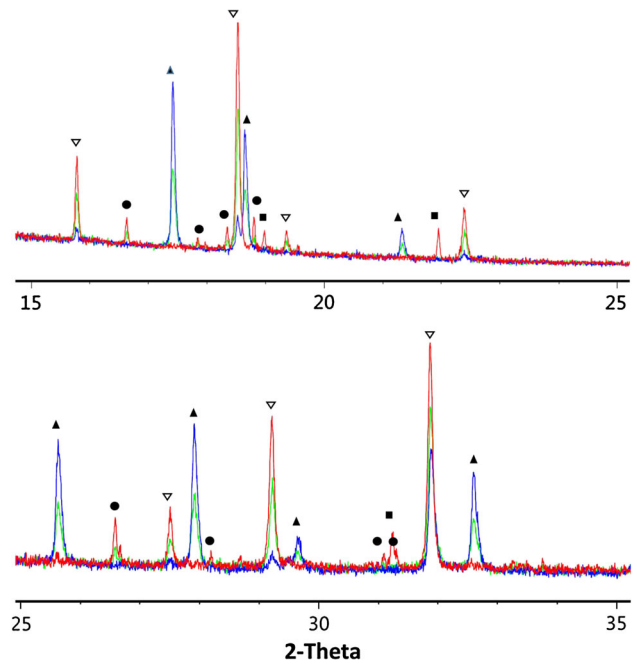


Fig. 4—Peak changes during reduced iron ore oxidation: sample OC2 at 1223 K (950 °C) for 3 min (red), after 12 min (green), and after 33 min (blue). Legend: filled up pointing triangles Fe_2O_3 , open down pointing triangles Fe_3O_4 , filled squares FeO , filled circles Fe_2SiO_4 (Color figure online).

IV. DISCUSSION

Previously, we estimated the kinetics of iron ore and ilmenite oxidation and reduction, with and without different ashes, using TGA measurements.^[7] In the

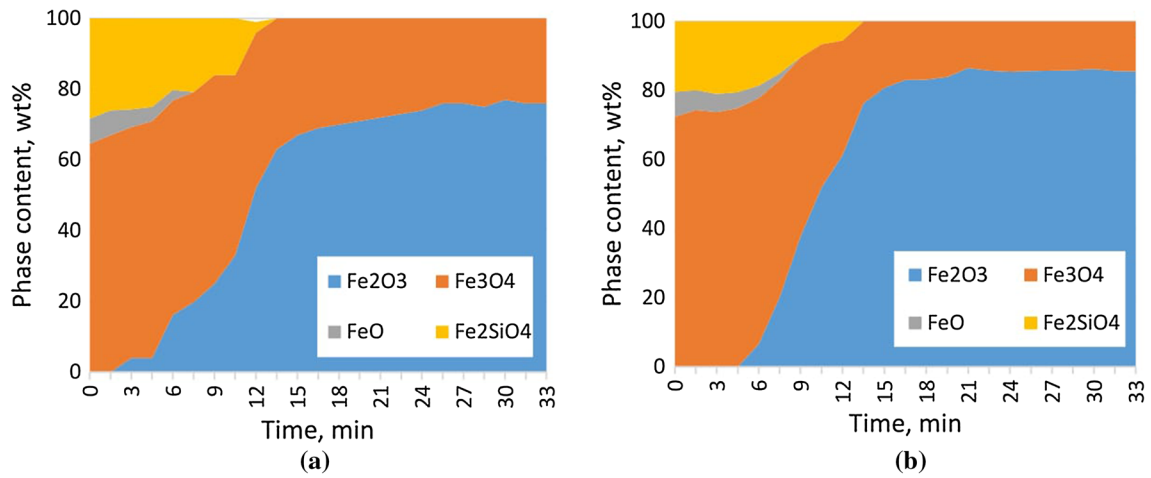


Fig. 5—Compositional changes in iron ore (sample OC2) during oxidation at 1223 K (950 °C) determined by HighScore (a) and by peak intensity (b).

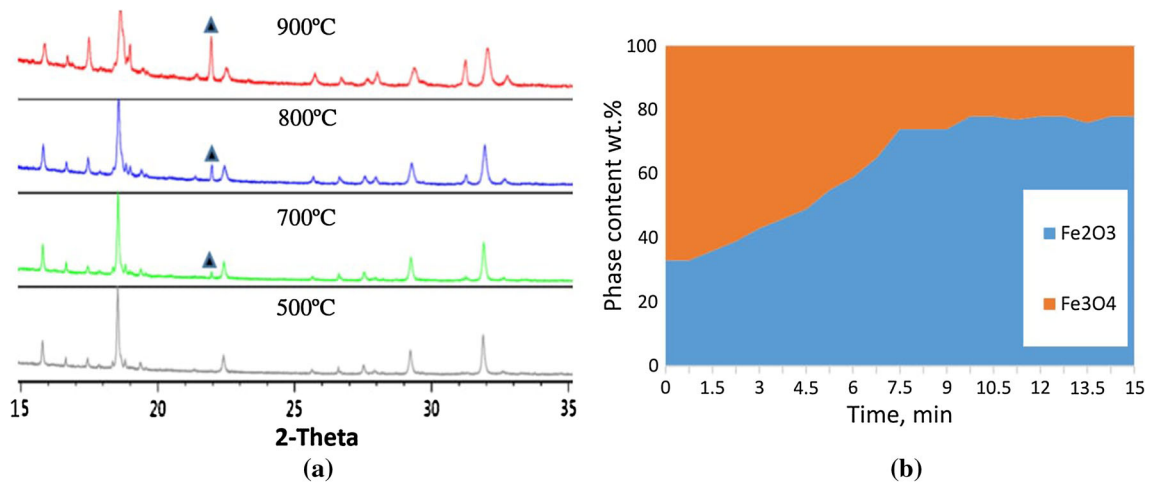


Fig. 6—XRD patterns in iron ore (sample OC2) during heating in N₂ at 773 to 1173 K (500 to 900 °C) (a) (marker shows hematite growth), and the compositional changes at 1223 K (950 °C) determined by HighScore (b).

present study, the reduction of calcined iron ore was significantly affected by the limited amounts of carbon in the system. In the previous study, the iron ore and iron ore–ash mixtures initially heat treated in air (oxidized) were directly exposed to CO in the atmosphere. In the present study, a reaction between carbon and oxygen from oxide would have to occur before the reactions of gases with carbon and the formation of CO₂. Therefore, the kinetics of the phase transformation was expected to be slower.

Most of the oxidation transformations (mainly reaction (3)) occurred in the OC2 sample in 10 minutes (within 3 to 13 minutes of exposure to air), according to Figure 5, which is slightly longer than the 7 to 8 minutes in a similar conversion observed by oxidation in a TGA reactor.^[7] This could be because of the presence of the fayalite phase, which appeared due to higher silica content in the OC2 iron ore. However, in general, both

trends are very similar and correspond to other studies on magnetite oxidation,^[17] where magnetite exponentially lost about 80 pct of the fraction in 5 minutes during oxidation at 1173 K (900 °C). In the presence of ash, the oxidation of iron ore–ash mixture in a TGA reactor is completed in 5 minutes, which is even faster than pure iron ore oxidation. The phase transformations in air of partially oxidized iron ore in powder diffraction capillary were mainly completed in 10 minutes (Figures 5(a) and (c)). The fact that the material was not completely reduced in the reduction step and was partially converted to hematite may explain this difference.

Thermodynamic calculations demonstrate that ilmenite transforms to rutile and pseudobrookite in oxidation step (Reaction [4]), and then at the reduction step the pseudobrookite converts to rutile, ilmenite, and magnetite (Reaction [5]), which should be transformed

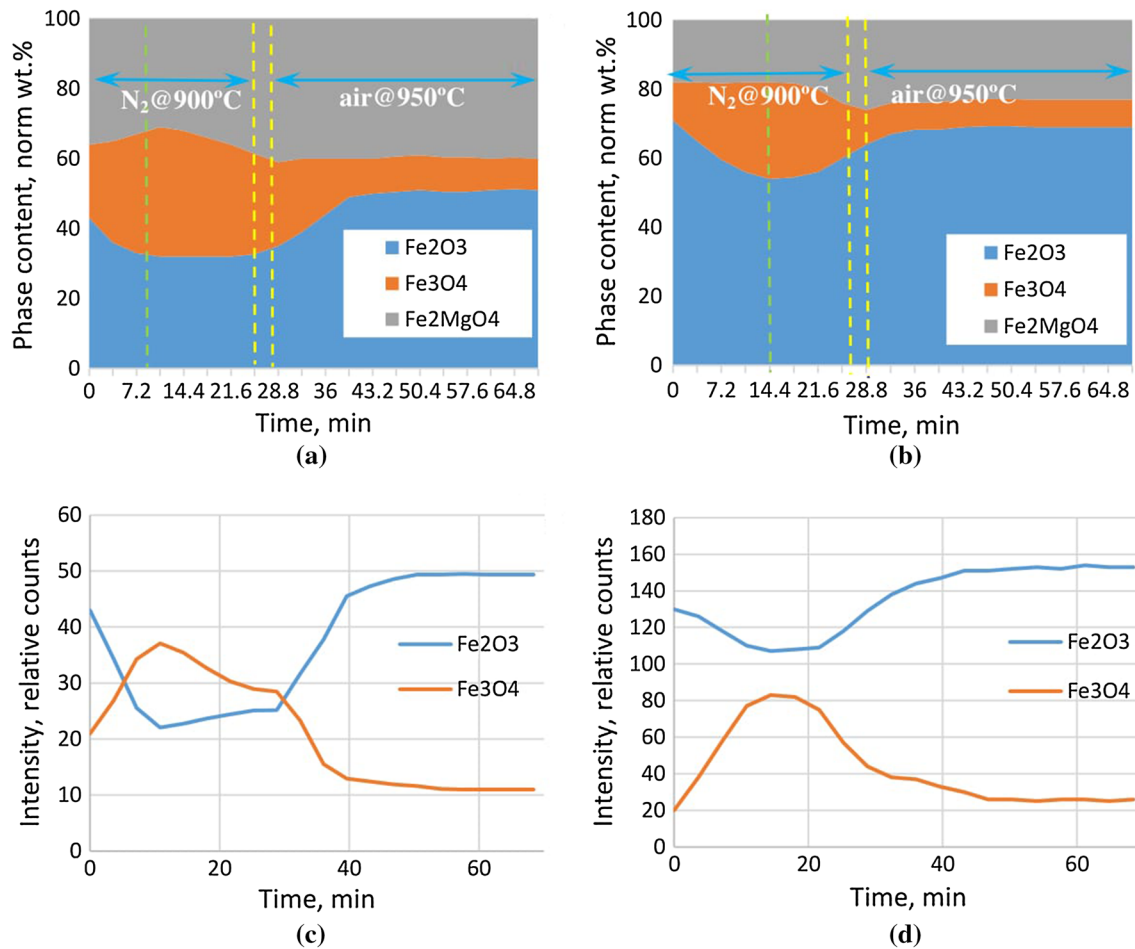


Fig. 7—Phase changes in OC1 (a, c) and OC2 (b, d) during reduction and oxidation, calculated by HighScore (a, b) and peak intensities (c, d).

back to pseudobrookite under oxidizing conditions (Reaction [6]).^[8] However, in the observed reactions, the oxidation was stopped, and pseudobrookite did not reach the initial content, but the hematite concentration was fluctuating slightly above the initial value.

According to the mass gain trends for the mixture of ilmenite with silica-rich ash, more than 90 pct of the material reduced after 30 minutes and oxidized in just 7 to 8 minutes. Without ash, calcined ilmenite reached 90 pct of reduction in 15 minutes and then the reduced material was 90 pct oxidized in 5 minutes. Similar to iron ore reduction, comparing the ilmenite reduction kinetics with the previous TGA study is difficult because of the limited amount of carbon and no direct reaction with CO.

Transformations of phases during ilmenite oxidation also occur slower than under TGA conditions. However, the trends shown in Figures 9 and 10 demonstrate that certain amount of already oxidized material exists in hematite form, and the complete recovery of ilmenite–hematite–rutile mixtures to pseudobrookite may take a much longer time. This means that in a CLC system working with ilmenite as OCs, some material will follow magnetite–hematite reversible transformations. This supports other studies on ilmenite redox and oxidation in CLC, where it was observed that

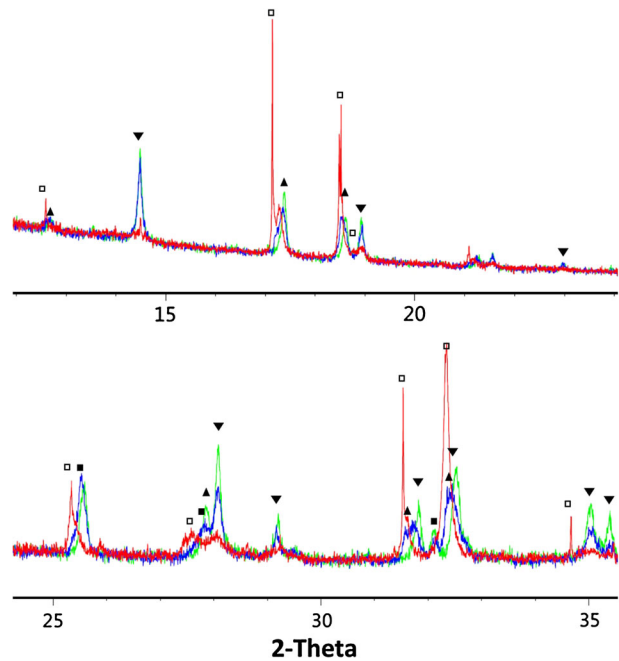


Fig. 8—XRD patterns of OC3 taken at the beginning of calcination (green), after 12 min (blue) and after 25 min (red). Legend: open squares FeTiO_3 , filled squares Fe_2TiO_5 , filled down pointing triangles TiO_2 , and filled up pointing triangles Fe_2O_3 .

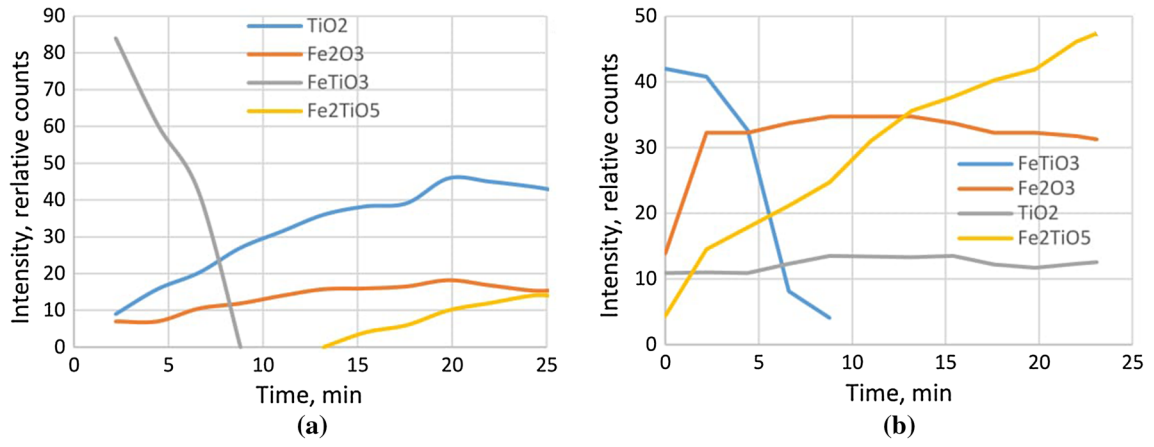


Fig. 9—Changes in peak intensities of the phases in sample OC3 during initial oxidation (a) and oxidation (b) after reduction step.

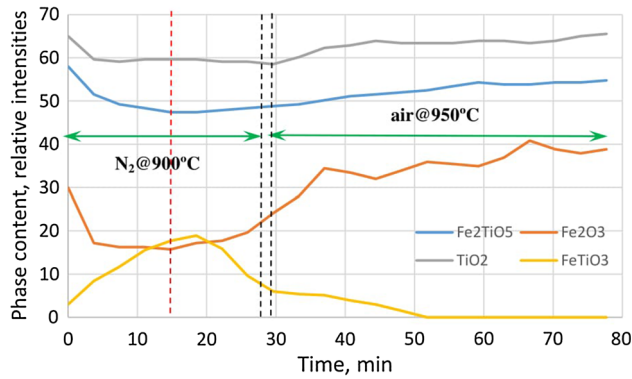


Fig. 10—Phase changes in OC3 during reduction and oxidation.

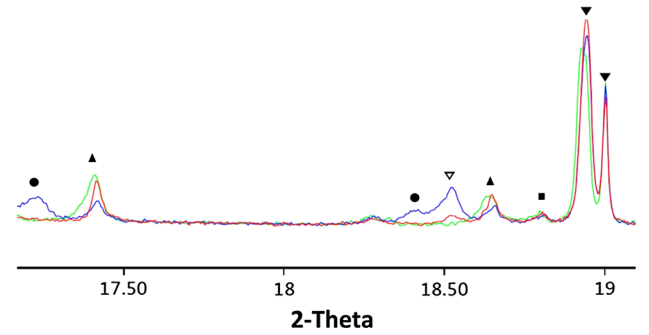


Fig. 12—Peak changes in sample OC3: red, just inserted into 1223 K (950 °C), blue, after 15 min at 1223 K (950 °C) (reduction step), green, after 60 min at 950 °C (30 min of oxidation). Legend: filled up pointing triangles Fe_2O_3 , open down pointing triangles Fe_2SiO_4 , filled circles FeTiO_3 , filled squares Fe_2TiO_5 , filled diamonds TiO_2 .

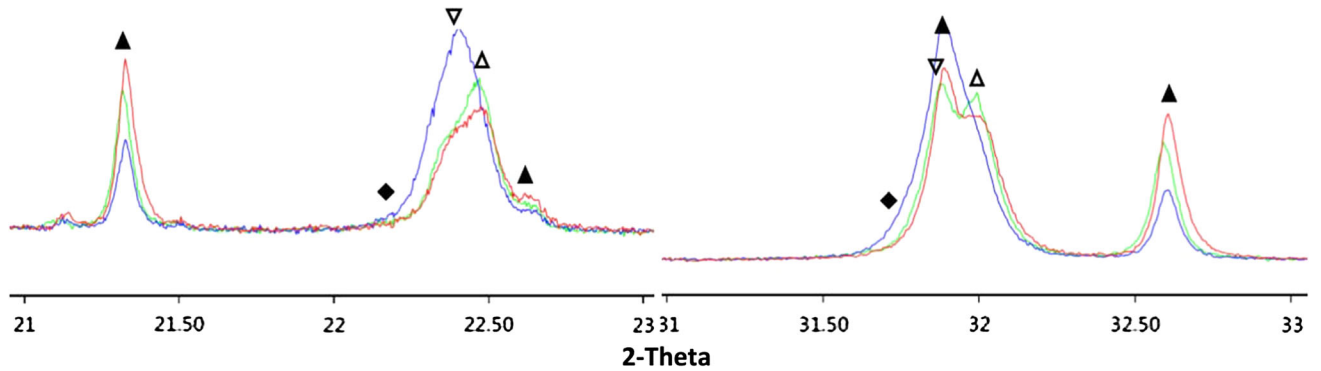
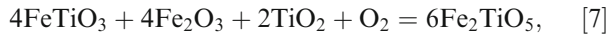
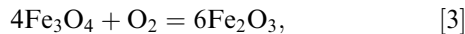


Fig. 11—Peak changes in sample OC1: red, just inserted into 1173 K (900 °C), blue, after 10 min at 1173 K (900 °C) (reduction step), green, after 10 min of oxidation. Legend: filled up pointing triangles Fe_2O_3 , open down pointing triangles Fe_2O_3 , open up pointing triangles Fe_2MgO_4 , filled diamonds MgO .

Fe_2O_3 appears on the external shell of ilmenite during the redox cycle due to migration of Fe^{2+} or Fe^{3+} ions.^[15] It may not recover hematite back to ilmenite, and this increase in the hematite fraction in the system

with increase of number of cycles, causing the attrition of ilmenite particles in the later stage.^[4]

Therefore, the mechanism of pseudobrookite oxidation was suggested to be:



where the migration of iron makes the second reaction slower.

V. CONCLUSION

In situ characterization of phase compositions in ilmenite and iron ore systems demonstrated the following specifics of the phase transitions and mechanism of the reaction:

- Initial oxidation of both OCs quickly transforms the goethite fraction of iron ore to hematite, and ilmenite phase of ilmenite to rutile, pseudobrookite, and hematite.
- In reducing atmosphere, hematite iron ore in iron ore converts to magnetite, while ilmenite reduction leads to ilmenite phase growth that coexists with some amounts of hematite, rutile, and titanium magnetite.
- During the oxidation of reduced iron ore, the wustite and fayalite phases disappear first, followed by hematite growth and then the decreasing of the magnetite phase.
- During reduced ilmenite oxidation, magnetite disappears first and then reacts with ilmenite to form ilmenite–hematite solution with stoichiometry $\text{Fe}_{1.35}\text{Ti}_{0.65}\text{O}_3$. Then, ilmenite–hematite transforms to pseudobrookite and hematite, with continued crystallization of pseudobrookite with hematite consumption.

Under reducing atmosphere, the changes in peak ratio of iron ore–ash mixture indicate a reaction between magnetite and magnesio-ferrite, while in the ilmenite–ash mixture, ilmenite–silica interaction was observed as fayalite phase growth.

VI. ACKNOWLEDGMENTS

This research is supported by the Science and Industry Endowment Fund. The authors acknowledge the facilities and technical assistance of Powder Diffraction Beamline (Proposal AS153/PD/10019) at the Australian Synchrotron, Victoria, Australia.

REFERENCES

1. M.M. Hossain and H.I. de Lasa: *Chem. Eng. Sci.*, 2008, vol. 63, pp. 4433–51.
2. J. Adanez, A. Abad, F. Garcia-Labiano, P. Gayan, and L.F. de Diego: *Prog. Energy Combust. Sci.*, 2012, vol. 38, pp. 215–82.
3. Q. Imtiaz, D. Hosseini, and C.R. Müller: *Energy Technol.*, 2013, vol. 1, pp. 633–47.
4. F. Mayer, A.R. Bidwe, A. Schopf, K. Taheri, M. Zieba, and G. Scheffknecht: *Appl. Energy*, 2014, vol. 113, pp. 1863–68.
5. A. Cuadrat, A. Abad, J. Adánez, L.F. de Diego, F. García-Labiano, and P. Gayán: *Fuel Process. Technol.*, 2012, vol. 94, pp. 101–12.
6. R. Xiao, L. Chen, C. Saha, S. Zhang, and S. Bhattacharya: *Int. J. Greenh. Gas Control*, 2012, vol. 10, pp. 363–73.
7. A. Ilyushechkin, M. Kochanek, and S. Lim: *Proc. 2015 ICCS&T*, 2015.
8. A. Ilyushechkin, M. Kochanek, and S. Lim: *Fuel Process. Technol.*, 2016, vol. 147, pp. 71–82.
9. A.F. Gualtieri and P. Venturelli: *Am. Mineral.*, 1999, vol. 84, pp. 895–904.
10. A. Cheung, W. Eu, and M. Valix: *Proc. XXIV Int. Miner. Process. Congr.*, 2008, vol. 2, pp. 2986–91.
11. W. Eu, A. Cheung, and M. Valix: *J. Synchrotron Radiat.*, 2009, vol. 16, pp. 842–48.
12. S. Rajendran, S. Zhang, R. Xiao, and S. Bhattacharya: *Proc. Combust. Inst.*, 2015, vol. 35, pp. 3619–27.
13. T. Degen, M. Sadki, E. Bron, U. König, and G. Nénert: *Powder Diffr.*, 2014, vol. 29, pp. S13–S18.
14. H. Naono, K. Nakai, T. Sueyoshi, and H. Yagi: *J. Colloid Interface Sci.*, 1987, vol. 120, pp. 439–50.
15. J. Adanez, A. Cuadrat, A. Abad, P. Gayan, L.F. de Diego, and F. Garcia-Labiano: *Energy Fuels*, 2010, vol. 24, pp. 1402–13.
16. University of Cambridge: <http://www.doitpoms.ac.uk/tlplib/xray-diffraction/peak.php>, 2016 (accessed 12.09.16).
17. A.R. Firth and J.F. Garden: *Metall. Mater. Trans. B*, 2008, vol. 39B, pp. 524–33.